Applied Computer Science, vol.19, no.1, pp. 133–151
doi: 10.35784/acs-2023-09

Submitted: 2023-02-23 | Revised: 2023-03-09 | Accepted: 2023-03-11

Keywords: Cooperative robotic system, Handling force, MANFIS controller, object-tool contact.

Abderrahim BAHANI [0000-0002-6794-2487]*, El Houssine ECH-CHHIBAT*, Hassan SAMRI*, Hicham AIT EL ATTAR* , Laila AIT MAALEM*

Department of Mechanical Engineering, ENSET Mohammedia, Hassan II University of Casablanca, Morocco.

INTELLIGENT CONTROLL OF THE GRIPPING FORCE OF AN OBJECT BY TWO COMPUTER-CONTROLLED COOPERATIVE ROBOTS

Abstract:

This paper presents a method based on Multiple Adaptive Neuro-Fuzzy Inference System (MANFIS) to regulate the handling force of a common object. The foundation of this method is the prediction of the inverse dynamics of a cooperative robotic system made up of two 3-DOF robotic manipulators. Considering the lack of slippage in the contact between the tool and the object, the object is moved. To create and feed the MANFIS database, the inverse kinematics and dynamic equations of motion for the closed chain of motion for both arms are established in Matlab. Results from a SimMechanic simulation are given to demonstrate how well the suggested MANFIS controller works. Several manipulated object movements covering the shared work-space of the two manipulator arms are used to test the proposed control strategy. The simulation results indicate that the proposed control strategy is effective in regulating the handling force of a common object with varying desired forces, and does not require the use of force sensors on the object-tool contact.

1. INTRODUCTION

Modern automated production is increasingly using three-degree-of-freedom (3-DOF) robot manipulators that are affordable. The use of manipulator control, analysis of cinematic content, analysis of the dynamic behavior of multiple robot manipulators, and mathematical modeling tasks are pertinent and important. Numerous academic articles examine the modeling strategies used by cinematic, dynamic, and multilink robot manipulators. For instance, Liu et al. (2017) and Arian et al. (2017) both perform mathematical modeling of the cinematic and dynamic behavior of the 3-DOF Gantry-Tau manipulator. Along with the cinematic analysis of the manipulator, the problems with trajectory planning and transformation are also covered.

The filming of a three-link manipulator used in the automotive industry is examined in the article (Herrero et al., 2018). The ability of cooperative robot systems to move and manipulate objects is their main advantage. Robots can cooperate with one another using these systems to complete tasks. In other words, multiple robots can move the object, where

a single robot cannot, by sharing the load or burden among them. Cooperative robots can handle multiple objects simultaneously while performing assembly tasks, lengthening the procedure and removing the requirement for a specific environment.

As for the autonomous actions of the robot, several control strategies specifically determine the movement of the object. Robotic arms perform independent actions that alter the trajectory of the object into the trajectories of each of their effectors. Hybrid control schemes for the position, force and coordination of multiple robotic arms have also been developed. The use of forcefully coordinated multiple robotic arms has been suggested in the literature (Hayati, 1986). For a multi-robot system performing assembly tasks, the coordinated law of command also includes internal and external movement control (Hsu, 1989).

Many adaptive control schemes for coordinated arms have not taken into account the effects of uncertainties in dynamic models (Hu & Goldenberg,1989; Walker et al, 1989). The majority of the proposed methods may have problems with their ability to control processes if the effects of perturbation and uncertainty are not taken into account. These are the problems with most of the controllability of the proposed methods. Recently, manipulator control has been carried out using robust adaptive and variable structure control systems that are built to overcome uncertainty in the presence of disturbances. Perturbation has recently been used for manipulator control (Azadi et al., 2005), and it can also be used for the hands of cooperative robots.

The use of artificial intelligence in industrial robotics has increased over the past few decades but closed robotic systems have not incorporated ANFIS much outside of Bahani et al. (2022) and Han et al. (2023)'s work on the kinematics modeling of the ambidextrous arm.

In particular, the ANFIS is used in this work to develop a multiple intelligent robot engine driver that can control a complex non-linear system made up of two flexible jointed manipulators handling a single object. The functions it must perform include trajectory tracking, enhancing grip force, eradicating vibratory behavior, and disturbance rejection. As the purpose of this work lies at the intersection of the fields of robotics and control, we have chosen the following organisational structure for it. The method proposed in this article allow us to create computer-assisted robots as shown in Figure 1 and instead of relying on non-linear algebraic equations for control we can use artificial intelligence algorithms for control.

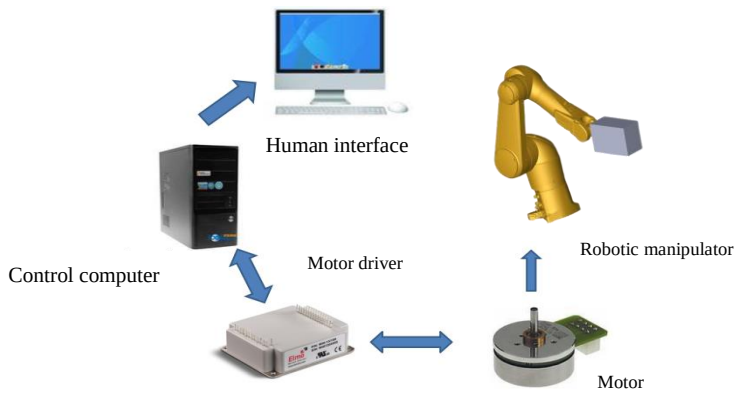

Fig. 1. Computer-controller manipulator robot

2. PROBLEM MODELING

2.1. Preliminary

To create an overall system dynamic model, imagine a body that is controlled by two robots, to which a frame of non-inertial coordinates Σ_O with the origin at the mass center of the object is attached, to mathematically describe the object's motion (Figure 2).

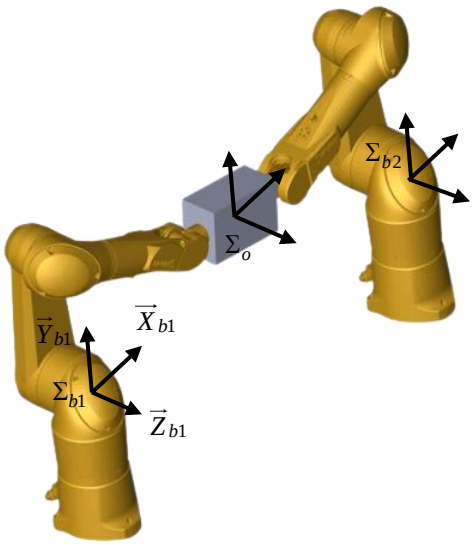

Fig. 2. A three-DOF modeling of two cooperative robots

2.2. Assumptions

The following presumptions are made (Kawazaki et al., 2003) to help with the dynamic formulation (Ivanov et al, 2020).

A1: Each robot arm has a unique number of axes since none of the robot arms are redundant.

A2: The desired position of the object, the desired velocity and the desired manipulative force are time-determined and limited;

A3: To prevent relative motion between the object and the end effector, which could produce an arbitrary force and moment at the point of contact, all robot end effectors are rigidly linked to the shared object.

The control goal is to propose an ANFIS robot engine driver for each manipulator so that all signals of the manipulator's global cooperative system remain uniformly bound, the object moves along a desired position and orientation trajectory, and internal forces and torques reach the desired values.

3. DYNAMICS MODEL OF THE COMPLETE SYSTEMS

3.1. Dynamics of the object

An object's motion is represented by the shift in the coordinate frame's position with respect to the inertial frame. If the "clamped-clamped" model is used, the center of mass of the rigid body can be determined using the vectors $r_{0,1}$ and $r_{0,2}$ in the object frame.

We may specify:

$$X_i = \begin{bmatrix} P_i^T & \theta_i^T \end{bmatrix}^T \quad i = 1,\ 2 \tag{1}$$

Represents the pose of the (i =1, 2) end effector on the ith robot. P_i is a (3×1) vector that is given by (Azadi et al., 2005):

$$P_i = P_0 + R_{0,b}(\theta) r_{0,i} \quad i = 1,\ 2 \tag{2}$$

Where P_0 denotes the object's mass center's position vector, $R_{0,b}(\theta)$ denotes the body frame's rotation matrix with respect to the inertial frame, and $r_{0,i}$ denotes the end-effector i's position vector in the body frame. The ith end-orientation effector's vector, $\theta_i(3\times1)$, is provided by:

$$\theta_i = \theta + \theta_{0,i} \quad i = 1,\ 2 \tag{3}$$

Where the orientation of the object frame (O-xyz) with respect to the inertial frame is denoted by $\theta_{0,i}$ and θ is an orientation vector corresponding to the initial configuration of the end effector i.

Combining Eqns. (2) and (3), we get the following result by setting $x_0 = \begin{bmatrix} P_0^T & \theta^T \end{bmatrix}^T$ as the object's position/orientation vector:

$$X_i = x_0 + \begin{bmatrix} R_{0,b}(\theta) r_{0,b} \\ \theta_{0,i} \end{bmatrix} \quad i = 1,\ 2 \tag{4}$$

By dividing Equation (4), we obtain:

$$\dot{X}_i = \begin{bmatrix} \dot{P}_0 \\ \dot{\theta} \end{bmatrix} + \begin{bmatrix} \dot{R}_{0,b}(\theta) r_i^0 \\ 0 \end{bmatrix} \quad i = 1,\ 2 \tag{5}$$

Equation (5) can be rewritten as follows:

$$\dot{X}_i = R_{0_i}(\theta).\dot{x}_0 \quad i = 1,\ 2 \tag{6}$$

where:

$$R_{0_i}(\theta) = \begin{bmatrix} I_{3\times3} & A_i(\theta, r_{0,i}) \\ 0_{3\times3} & I_{3\times3} \end{bmatrix} \quad i = 1,\ 2 \tag{7}$$

where $I_{3\times3}$ and $0_{3\times3}$ are, respectively, the identity and zero matrices for the third dimension, and:

$$A_i(\theta, r_{0,i})\dot{\theta} = \frac{dR_{0,b}(\theta)}{dt} r_{0,i} \quad i = 1,\ 2 \tag{8}$$

Let $J_{A_i}(q_1)$ be the Jacobian matrix for robot i and let q_i be the vector of joint displacements. We get the following equation by defining $X_i = \begin{bmatrix} q_1{}^T & q_2{}^T & x_0{}^T \end{bmatrix}^T$ as the combined coordinate vector:

$$J(x)\dot{x} = 0 \tag{9}$$

where $J(x)$ is the full system's Jacobian matrix, denoted by:

$$J(x) = \begin{bmatrix} J_{A_1}(q_1) & 0_{6\times n} & -R_{0_1}(\theta) \\ 0_{6\times n} & J_{A_1}(q_2) & -R_{0_1}(\theta) \end{bmatrix} i = 1,\ 2 \tag{10}$$

where *n* denotes a single robot's degrees of freedom.

3.2. Manipulator dynamics

The dynamic equations of the robot motion with respect to joint coordinates are obtained using Newton-Euler dynamics (Azadi et al., 2005):

$$H_i(q_i)\ddot{q}_i + B_i(q_i, \dot{q}_i)\dot{q}_i + G_i(q_i) = \tau_i + J_{A_i}{}^T F_i \quad i = 1,\ 2 \tag{11}$$

where $G_i(q_i)$ is the vector of gravitational terms, $H_i(q_i)$ is the robot inertia matrix, $B_i(q_i, \dot{q}_i)$ is the matrix of Coriolis and centrifugal effects, and F_i is the generalized joint torque/force. Where F_i denotes the force/moment vector that the payload, as measured at the origin of the end-effector frame and expressed in the base frame of the robot i exerts on end-effector i.
Equation (11) can be rewritten as to.

$$\ddot{q}_i = H_i{}^{-1}(q_i)(\tau_i - \tau_i{}') \quad i = 1,\ 2 \tag{12}$$

where $\tau_i{}'$ represents the torque contribution that varies with joint positions and velocities:

$$\tau_i{}' = B_i(q_i, \dot{q}_i)\dot{q}_i + G_i(q_i) + J_{A_i}{}^T F_i \quad i = 1,\ 2 \tag{13}$$

3.3. Common-object dynamic

Lagrange's method is based on the calculation of the kinetic energy of each arm constituting the robot, this kinetic energy E_c is given by the relation:

$$E_c = \frac{1}{2}\left[mv^T v + \omega^T I_W \omega \right] \tag{14}$$

where I_W is symmetric and represents the inertia tensor relative to the center of mass of the object when expressed in the inertial frame, and m is the object's mass, v is the linear velocity of the center of mass, ω and is the body's angular velocity. The object's potential energy is :

$$U = mgy_0 \tag{15}$$

where y_0 is the center of mass's z coordinates in the inertia frame and g is the gravitational constant. The object's Lagrangian is as follows:

$$L = E_c - U = \frac{1}{2}\left[mv^T v + \omega^T I_W \omega \right] - mgy_0 \tag{16}$$

The power supplied by external forces and torques must be equal to the power supplied by the generalized forces in the object's mass, so:

$$-f_1^T V_1 - f_2^T V_2 = F^T V_0 \tag{17}$$

where f_1 and f_2 are the forces and moments that the object applied to each the robots 1, 2 measured at the end effectors frame's origin and expressed in these frames, and V_1, V_2 , and V_0 stand for the end effectors 1, 2, and object's respective velocity vectors. In what way $\dot{X}_{R,E}$ and $\dot{q}$ relate by:

$$\dot{X}_{R,E} = J_f \dot{q} \quad \text{where } J_f = T_{fr}^{-1} J_A \tag{18}$$

and T_{fr} is an identity matrix for RPY angles.

When we consider the relation (18) and replace equation (6) in equation (17), we get:

$$(-f_1^T T_{fr1} R_{O_1} - f_2^T T_{fr2} R_{O_2})\dot{x} = F^T T_{fr0} \dot{x} \tag{19}$$

when we solve Equation (20) for F, we get:

$$F = -T_{fr0}^{-T} \left(\sum_{i=1}^{2} R_{O_i}^T T_{fr_i}^T f_i \right) \tag{20}$$

We can obtain the dynamics of an object in the inertia frame by substituting Equations. (16) and (20) in the Lagrange formulation (Azizian, 2001; Azadi et al., 2005):

$$H_O(x_O)\ddot{x}_O + B_0(x_O, \dot{x}_O)\dot{x}_O + g_O = -\left(\sum G_{Wi} R_{rbi}^R F_i \right) i = 1,\ 2 \tag{21}$$

Where:

$$H_O(x_O) = T_{fr_O}^T M_{O,W} T_{fr_O} \tag{22}$$

$$M_{O,W} = \begin{bmatrix} M \times I_{3\times3} & O_{3\times3} \\ O_{3\times3} & I_W \end{bmatrix} \tag{23}$$

$$g_O = \begin{bmatrix} 0 & Mg & 0 & 0_{1\times3} \end{bmatrix} \tag{24}$$

$$G_{Wi} = T_{f_0}^{-T} R_{O_i}^T T_{fr_i}^T \tag{25}$$

and

$$R_{R,rb_i} = \begin{bmatrix} R_{b_i}^R & 0_{6\times6} \\ 0_{6\times6} & R_{b_i}^R \end{bmatrix} \tag{26}$$

where R_{R,rb_i} represents the rotation matrix of base frame i with respect to the inertial frame. and O stand i for object and ith robot, respectively, in the definitions of F_i and T_{fr} that were just given.

3.4. Complete systems dynamic

Two robots each holding a rigid payload make up the entire system, and their dynamic equation of motion is:

$$D(x)\ddot{x} + C(x,\dot{x})\dot{x} + G(x) = u + J_f^T(x) f \tag{27}$$

$$D(x) = \begin{bmatrix} H_1(q_i) & 0_{3\times3} & 0_{3\times3} \\ 0_{3\times3} & H_2(q_i) & 0_{3\times3} \\ 0_{3\times3} & 0_{3\times3} & H_O(x_O) \end{bmatrix} \tag{28}$$

$$C(x,\dot{x}) = \begin{bmatrix} B_1(q_1,\dot{q}_1) & 0_{3\times3} & 0_{3\times3} \\ 0_{3\times3} & B_2(q_2,\dot{q}_2) & 0_{3\times3} \\ 0_{3\times3} & 0_{3\times3} & B_O(x_O,\dot{x}_O) \end{bmatrix} \tag{29}$$

$$G(x) = \begin{bmatrix} G_1(q_1) \\ G_2(q_1) \\ g_O \end{bmatrix} \tag{30}$$

$$u = \begin{bmatrix} \tau_1 \\ \tau_2 \\ 0_{3\times3} \end{bmatrix}, f = \begin{bmatrix} f_1 \\ f_2 \end{bmatrix} \tag{31}$$

And

$$J_f = \begin{bmatrix} J_{A_1} & 0_{6\times3} & -R_{W,t1}{}^T R_{rb1}^T G_{W1}^T \\ 0_{6\times3} & J_{A_2} & -R_{W,t2}{}^T R_{rb2}^T G_{W2}^T \end{bmatrix} \quad (32)$$

4. CONTROL OF COOPERATIVE ROBOTS

4.1. Control cooperative robots

Intuition in mechanical engineering suggests using an inverse dynamics control of the form to cancel nonlinear terms and decouple the dynamics of each link.

$$\tau_i = H_i(q_i)\ddot{q}_i + B_i(q_i, \dot{q}_i)\dot{q}_i + G_i(q_i) - J_{A_i}{}^T F_i \quad (32)$$

which was used with Equation (11), and considering the regularity of the symmetric positive definite matrix $H_i(q_i)$, which verifies following Equation:

$$\lambda_m.I \le H_i(q_i) \le \lambda_M.I \quad (33)$$

The end result is a set of n coupled linear systems, where λ_m et λ_M denotes the exact minimum (maximum) strictly positive value of $H(q)$ for each configuration.

4.2. Intelligent control of cooperative robots

Due to the benefits that these tools provide, particularly for nonlinear systems, the control based on artificial intelligence represents a very large and active research field. It is based on the exploitation of these capacities of learning, approximation, and optimization that characterize these tools, among which we quote the artificial neural networks, the fuzzy logic, and the genetic algorithms.

The drivers of each manipulator robot receive instructions from the MANFIS controller as shown in the following figure 3:

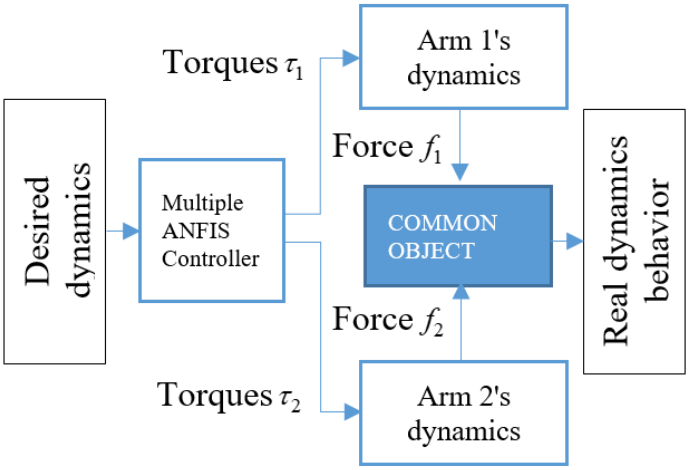

Fig. 3. Intelligent robot robot engine driver block diagram for robot (i)

5. ESTIMATION AND OPTIMIZATION OF THE EFFORT DISTRIBUTION ON THE OBJECT

The formulation and solution of the contact distribution is a problem which requires consideration. The following constraints must be taken into account in the formulation and solution of the contact distribution problem:

- Preventing the manipulated object from sliding while being held by a cooperative multi-robot system;
- Gradually varying the contact forces when the robots come into contact with the manipulated object to ensure a permanent contact when the object is held by the end effectors of the various robots. Most studies substitute an inequality for the friction cone in order to avoid the non-linearity of this equation (Mahfoudi et al., 2003).

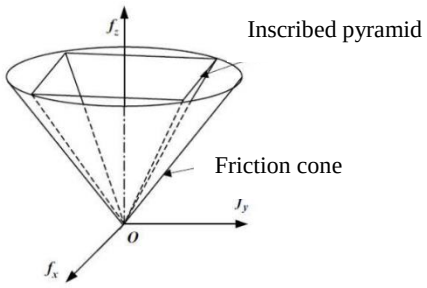

Fig. 4. The cone's inscribed pyramid of friction

$$f_y \leq \mu' f_z \tag{33}$$

with

$$\mu' = \frac{\sqrt{2}}{2}\mu \tag{34}$$

μ' represents is for the inscribed pyramid and μ .

The phenomenon of sliding on the contact surface when the object is held by the end effectors of the cooperative robots, can be reduced by maximizing the ratio of forces acting on the robots' tangential and normal components. By defining the overall ratio as the ratio between the normal and tangential force acting on the manipulated object, the authors (Klein & Kittivatcharapong, 1990) discovered a relationship connecting the forces on the robots and allowing the transformation of part of the friction problem from the nonlinear to the linear case.

The benefit of this approach is that some forces will satisfy the same global ratio of forces, while the remaining forces must satisfy the constraint inequalities determined by the previous equation. For those belonging to the second type, for instance, we get (Mahfoudi et al., 2003):

$$f_{x_i} = k_{xz} f_{z_i} \tag{35}$$

and

$$f_{x_i} \leq \mu^* f_{z_i} \tag{36}$$

With $k_{xz} = \frac{F_x}{F_z}$ is the overall ratio of the forces that were applied to the object being moved in accordance with the direction and

$$\mu^* = \sqrt{\mu^2 - {k_{xz}}^2} \tag{37}$$

6. TRAJECTORY AND FORCE GENERATION STRATEGY (MANFIS)

Fuzzy logic and neural networks are combined in the adaptive network fuzzy inference system (ANFIS), created by Jang in the 1990s (Jang, 1989), to create a hybrid intelligent system that automatically improves the capacity for learning and adaptation (Jha et al., 2015).

Researchers have used hybrid systems for modeling and forecasting across a range of te chnological fields (Esen et al., 2008).

The main objective of these adaptive techniques is to provide the modelling process with a fuzzy way of acquiring knowledge. Figure 5 depicts the five layers that make up the ANFIS structure.We will use a system with inputs (x1,, xn) and one output (y) to make things easi er to understand.

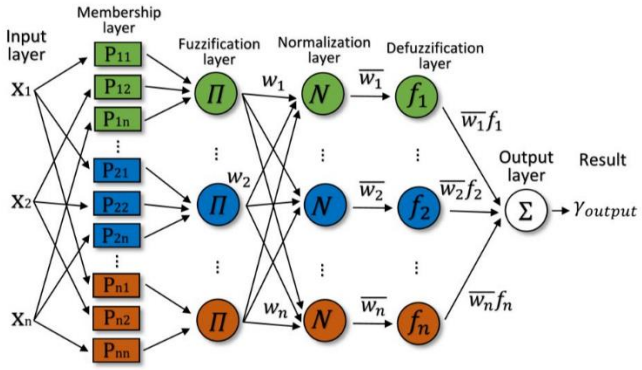

Fig. 5. The different layers of ANFIS

Adaptive Neuro Fuzzy Inference System is the full name of the system. It is a hybrid approach that makes use of neural network machine learning to create fuzzy logic. In order to learn the features or weights of a mathematical function from a given data set, neural networks are used. The data set is utilized for feature extraction and learning. As a result, a hypothesis is first developed for the parametrized mathematical model, and then the model is trained using the data. Since the calculations are less complicated and require less computational power, Forward Kinematics was used to create the data set in this case. The membership function of a fuzzy inference system of the Sugeno type is tuned by the neural network.

7. SIMULATION AND RESULTS

7.1. Simulation

Matlab/SimMechanic and SolidWorks simulations are used to model the kinematics and dynamics of the manipulated object.

- X and Y axis translations while maintaining a constant force of grip,
- circular translation of diameter 60 mm, while ensuring a constant gripping force,
- for the circular translation we vary the desired gripping force in a sinusoidal way and we take into account the errors made by the designed MANFIS robot engine driver s.

The authors discussed how to use a fuzzy robot engine driver to control a system in a way that respects the gripping force and enables the robot to follow an imposed trajectory. of the manipulated object with 5 kg of mass and his Moments of inertia $I_{ZZ} = 0.0009744 \text{kg.m}^2$. The desired handling force is 100 Newton.

The 3-DOF planar manipulator system for the proposed robot manipulator model (see Figure 9). The individual links' lengths are $L_1 = 0.225$ m $L_2 = 0.15$ m and $L_3 = 0.16$ m, as shown Figure 6. The dynamic characteristics of each of the robot arms are listed in the Table 1.

Tab. 1. The Dynamics Parameters of Robots

Link No.	Mass (kg)	Moments of inertia I_{ZZ} (kg·m²)
1	0.18724	0.00123677
2	0.113838	0.000315752
3	0.148558	0.000322059

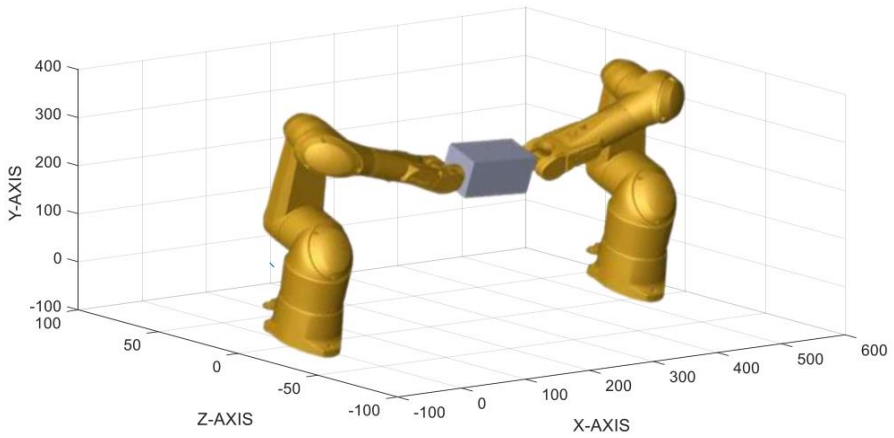

Fig. 6. The MATLAB/SimMechanic models for the three-DOF robots

The database from "Workspace" is the basis for the learning system, after solving the inverse dynamic of the set of cooperative robots. The Matlab scripts will feed each ANFIS robot engine driver whose structure is shown in Figure 7 below.

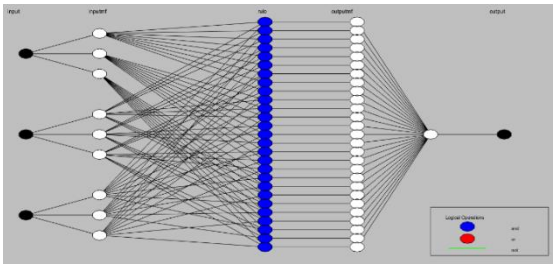

Fig.7. Training of ANFIS structure

The training of our fuzzy robot engine driver , which will be injected into the inverse model in figure 8, uses this database.

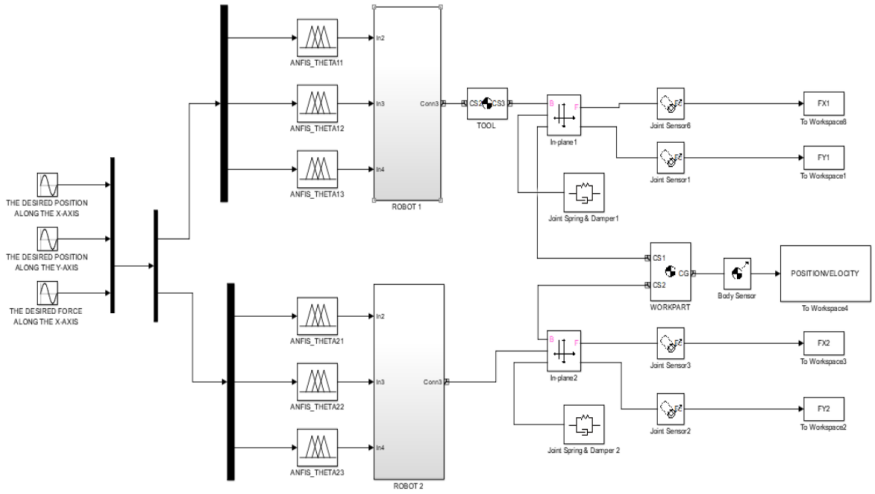

Fig. 8. Matlab/Simulink diagram of the milling system assembly with MANFIS robot engine driver

7.2. Results

We can control our robot by selecting a trajectory and gripping force after training the robot engine driver for each joint. We then compare this trajectory with those made using the fuzzy robot engine driver in Figures 9, 10, 11, 12, 13, 14, 15, 16, and 17.

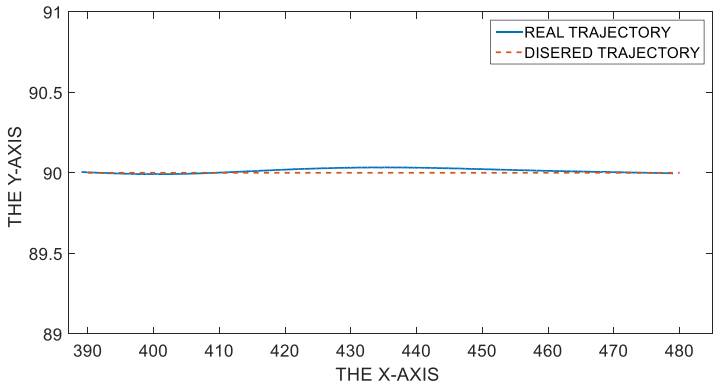

Fig. 9. Simulation results translation along the X-Axis in mm

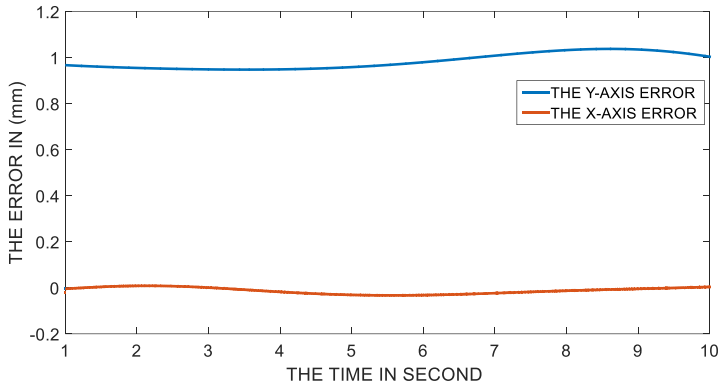

Fig. 10. The error committed during the linear trajectory along the X-axis, as a function of time in second

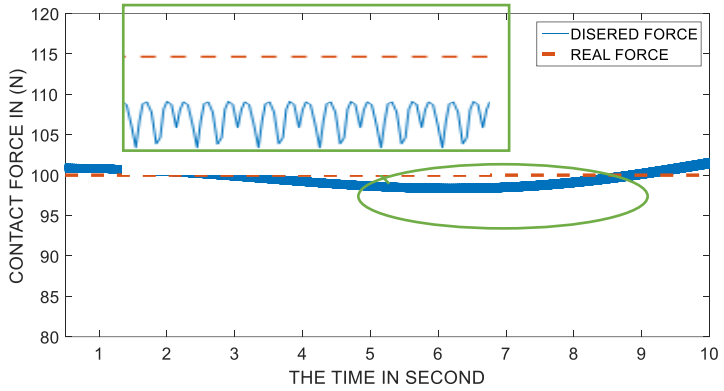

Fig. 11.Move along translation trajectory with constant desired handling force, as a function of time in second

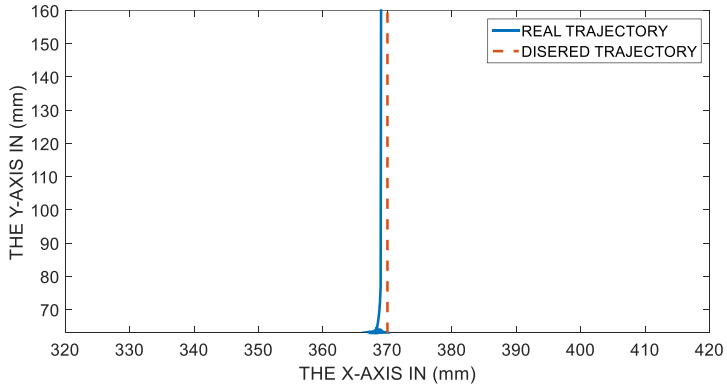

Fig. 12. Translation along the Y-Axis is the result of simulation

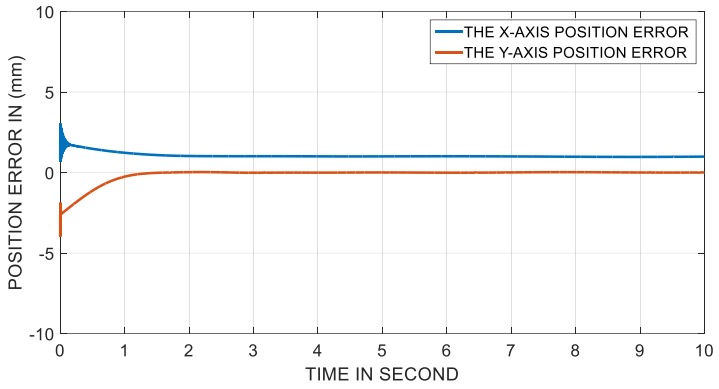

Fig. 13. The error committed during the linear trajectory along the Y-axis, as a function of time in second.

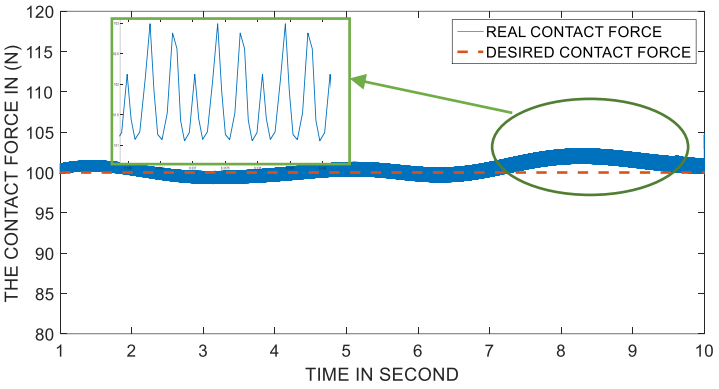

Fig. 14. Move along translation trajectory with constant desired handling force, as a function of time in second

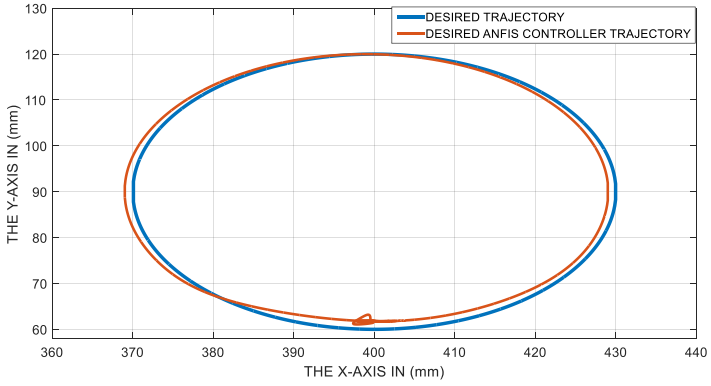

Fig.15.Move along circular trajectory with constant desired handling force

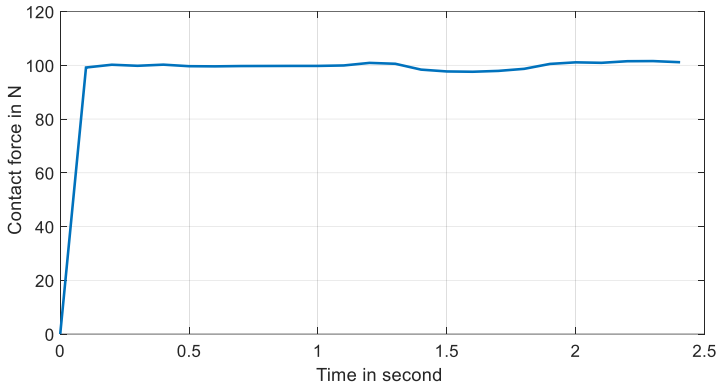

Fig. 16.Move along circular trajectory with constant desired handling force, as a function of time in second

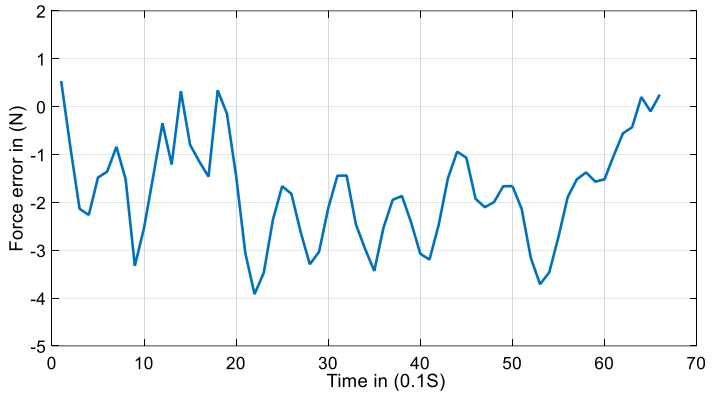

Fig.17.The common-object handling force error, as a function of time in (0,1*second)

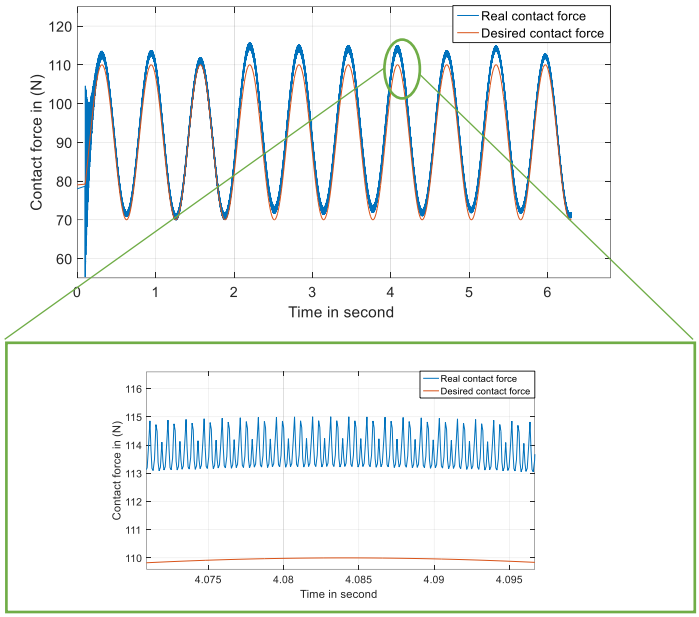

Fig. 18. Move along circular trajectory with variable desired handling force, as a function of time in second

7.3. Discussion

The simulation results demonstrate that even with a drive of no more than 100 epochs, the MANFIS robot engine driver is capable of reproducing the desired trajectories and gripping force. As shown in the figures, this robot engine driver made a position error of about 2 mm, which enables the validation of this method. We submitted this robot engine driver to the variable handling force as shown in Figure 16 to assess how it responded to the variation of the handling force for the handling force error between 1 and -4 Newton.

The outcomes demonstrate the effectiveness and precision of using MANFIS to regulate the grasping force of two robot manipulators. Even with varying setpoint forces, we were able to achieve prediction errors of less than 4%, which is on par with or even superior to the outcomes achieved with force control techniques described in the literature. This excellent performance is attributable to MANFIS's capacity to simulate in real time the intricate relationships between control inputs and input force outputs.

Although the results demonstrate the effectiveness and accuracy of using MANFIS to control the grasping force of two robot manipulators, it is crucial to critically assess and contrast them with other papers. The authors proposed a grasping force control method based on MANFIS that trains the control model in real-time using online learning techniques. Implementing this strategy is easy. However, other grasping force control techniques, including those based on neural networks, predictive control strategies, and hybrid force control techniques, have also been researched in the literature. These techniques have been used for a number of tasks, such as handling, polishing, and assembly. The MANFIS-based approach proposed by the authors has advantages over the previously

mentioned approaches. First off, it can speed up design and implementation because it does not call for elaborate modeling of the load properties. The MANFIS method is also resilient to load changes and capable of real-time disturbance adaptation. Last but not least, the strategy proposed by the authors makes use of an online learning algorithm to enable continuous updating of the control model, ensuring precision and stability of the force control. Furthermore, it does not require the implementation of force sensors on the contact between the manipulated object and the tool, which is the case in many previous research studies.

8. CONCLUSION

In conclusion, the authors of this paper proposed a MANFIS-based method, which proved to be accurate and effective, for controlling the gripping force of two 6-DOF robotic manipulators. The authors presented that the method is easy to use, adaptable in real time and can handle operational disturbances. With input force errors of less than 4% even when set point forces vary, the results show that using MANFIS to control input force significantly improves system performance. This demonstrates the versatility of the approach for a variety of applications requiring precise grip force control.

However, it is important to note that presented study has some limitations, such as using simulated data to train and test our control model. Therefore, future studies should be conducted to confirm the results experimentally and evaluate the applicability of the method to other systems.

To sum up, this study paves the way for further research to improve the grasping force control of manipulative robots. The authors believe that their method can be used to solve similar problems in the future and contribute to the advancement of industrial robotics.

Conflicts of Interest

The authors have no conflicts of interest to declare.

REFERENCES

Arian, A., Danaei, B., Abdi, H., & Nahavandi, S. (2017). Kinematic and dynamic analysis of the Gantry-Tau, a 3-DoF translational parallel manipulator. *Applied Mathematical Modelling*, *51*, 217-231. https://doi.org/10.1016/j.apm.2017.06.012

Azadi, M., Eghtesad, M., & Gharesifard, B. (2005). Inverse Dynamics Control of Two 5 DOF Cooperating Robot Manipulators. *Proceedings of the ASME 2005 International Design Engineering Technical Conferences and Computers and Information in Engineering Conference. Volume 4a: ASME/IEEE Conference on Mechatronic and Embedded Systems and Applications* (pp. 187-193). ASME. https://doi.org/10.1115/DETC2005-85634

Azizian, K. (2001). *Position control of two robots manipulating a rigid plate.* Shiraz University.

Bahani, A., Ech-Chhibat, E. H., Samri, H., & El Attar, H. A. (2022). Intelligent Modeling and Simulation of the inverse Kinematics Redundant 3-Dof Cooperative Using SolidWorks and MATLAB/Simmechanics. *International Journal on Technical and Physical Problems of Engineering (IJTPE)*, *50*(14), 78-88.

Esen, H., Inalli, M., Sengur, A., Esen, M. (2008). Artificial neural networks and adaptive neuro-fuzzy assessments for ground-coupled heat pump system. *Energy and Buildings*, *40*(6), 1074-1083. https://doi.org/10.1016/j.enbuild.2007.10.002

Han, J., Wang, F., & Sun, C. (2023). Trajectory Tracking Control of a Manipulator Based on an Adaptive Neuro-Fuzzy Inference System. *Applied Sciences, 13*(2), 1046. http://dx.doi.org/10.3390/app13021046

Hayati, S. (1986). Hybrid position-force control of multi arm cooperating robots. *Proceedings. 1986 IEEE International Conference on Robotics and Automation* (pp. 82-89). IEEE. https://doi.org/10.1109/ROBOT.1986.1087650

Herrero, S., Pinto, C., Altuzarra, O., & Diez, M. (2018). Analysis of the 2PRU-1PRS 3DOF parallel manipulator: kinematics, singularities and dynamics. *Robotics and Computer-Integrated Manufacturing, 51*, 63-72. https://doi.org/10.1016/j.rcim.2017.11.018

Hsu, P. (1989). Control of multi-manipulator system-trajectory tracing, load distribution, internal force control, and the decentralized architecture. *Proceedings, 1989 International Conference on Robotics and Automation* (pp. 1234-1239). IEEE. https://doi.org/10.1109/ROBOT.1989.100149

Hu, Y. R., & Goldenberg, A. A. (1989). An adaptive approach to motion and force control of multiple coordinated robots arms. *Proceedings, 1989 International Conference on Robotics and Automation* (pp. 1091-1096). IEEE. https://doi.org/10.1109/ROBOT.1989.100126

Ivanov, S., Meleshkova, Z., & Ivanova, L. (2020). Calculation and Optimization of Industrial Robots Motion. *2020 26th Conference of Open Innovations Association (FRUCT)* (pp. 115-123). IEEE. https://doi.org/10.23919/FRUCT48808.2020.9087376

Jang, J. S. R. (1993). ANFIS: Adaptive-Network-Based Fuzzy Inference System. *IEEE Transactions on Systems Man & Cybernetics, 23*(3), 665-685. https://doi.org/10.1109/21.256541

Jha, P., Biswal, B. B., & Sahu, O. P. (2015). Inverse Kinematic Solution of Robot Manipulator Using Hybrid Neural Network. *International Journal of Materials Science and Engineering, 3*(1), 31-38. https://doi.org/10.12720/ijmse.3.1.31-38

Kawazaki, H., Ito, S., & Ramli, R. B. (2003). Adaptative desentralised coordinated control of multiple robot arms. *IFAC robot control, 36*(17), 387-392. https://doi.org/10.1016/S1474-6670(17)33425-0

Klein, C. A., & Kittivatcharapong, S. (1990). Optimal force distribution for the legs of a walking machine with friction cone constraints. *IEEE Trans. on Robotics and Automation, 6*(1), 73–85. https://doi.org/10.1109/70.88119

Liu, F., Gao, G., Shi, L., & Lv, Y. (2017). Kinematic analysis and simulation of a 3-DOF robotic manipulator. *In 2017 3rd International Conference on Computational Intelligence & Communication Technology* (pp. 1-5). IEEE. https://doi.org/10.1109/CIACT.2017.7977291

Mahfoudi, C., Djouani, K., Rechak, S., & Bouaziz, M. (2003). Optimal force distribution forthe legs of an hexapod robot. *Proceedings of 2003 IEEE Conference on Control Applications* (vol.1, pp. 657-663). IEEE. https://doi.org/10.1109/CCA.2003.1223515

Walker, M.W., Kim, D., & Dionise, J. (1989). Adaptive coordinated motion control of two manipulators arms. *Proceedings, 1989 International Conference on Robotics and Automation* (pp. 1084-1090). IEEE. https://doi.org/10.1109/ROBOT.1989.100125